Available online at www.sciencedirect.com
ScienceDirect
Journal of Marine Systems 64 (2007) 66 – 88
JOURNAL OF MARINE SYSTEMS
www.elsevier.com/locate/jmarsys

# Validation of the 3D biogeochemical model MIRO&CO with field nutrient and phytoplankton data and MERIS-derived surface chlorophyll *a* images

Geneviève Lacroix [a,*], Kevin Ruddick [a], Youngje Park [a], Nathalie Gypens [b], Christiane Lancelot [b]

[a] *Management Unit of the North Sea Mathematical Models (MUMM), Royal Belgian Institute for Natural Sciences (RBINS), Gulledelle 100, 1200 Brussels, Belgium*

[b] *Ecologie des systèmes aquatiques (ESA), Université Libre de Bruxelles (ULB), Campus de la Plaine-CP 221, Boulevard du Triomphe, 1050 Bruxelles, Belgium*

Received 23 September 2005; received in revised form 20 December 2005; accepted 30 January 2006
Available online 20 July 2006

**Abstract**

This paper presents results obtained with MIRO&CO-3D, a biogeochemical model dedicated to the study of eutrophication and applied to the Channel and Southern Bight of the North Sea (48.5°N–52.5°N). The model results from coupling of the COHERENS-3D hydrodynamic model and the biogeochemical model MIRO, which was previously calibrated in a multi-box implementation. MIRO&CO-3D is run to simulate the annual cycle of inorganic and organic carbon and nutrients (nitrogen, phosphorus and silica), phytoplankton (diatoms, nanoflagellates and *Phaeocystis*), bacteria and zooplankton (microzooplankton and copepods) with realistic forcing (meteorological conditions and river loads) for the period 1991–2003. Model validation is first shown by comparing time series of model concentrations of nutrients, chlorophyll *a*, diatom and *Phaeocystis* with *in situ* data from station 330 (51°26.00′N, 2°48.50′E) located in the centre of the Belgian coastal zone. This comparison shows the model's ability to represent the seasonal dynamics of nutrients and phytoplankton in Belgian waters. However the model fails to simulate correctly the dissolved silica cycle, especially during the beginning of spring, due to the late onset (in the model) of the early spring diatom bloom. As a general trend the chlorophyll *a* spring maximum is underestimated in simulations. A comparison between the seasonal average of surface winter nutrients and spring chlorophyll *a* concentrations simulated with *in situ* data for different stations is used to assess the accuracy of the simulated spatial distribution. At a seasonal scale, the spatial distribution of surface winter nutrients is in general well reproduced by the model with nevertheless a small overestimation for a few stations close to the Rhine/Meuse mouth and a tendency to underestimation in the coastal zone from Belgium to France. $PO_4$ was simulated best; silica was simulated with less success. Spring chlorophyll *a* concentration is in general underestimated by the model. The accuracy of the simulated phytoplankton spatial distribution is further evaluated by comparing simulated surface chlorophyll *a* with that derived from the satellite sensor MERIS for the year 2003. Reasonable agreement is found between simulated and satellite-derived regions of high chlorophyll *a* with nevertheless discrepancies close to the boundaries.


*Keywords:* Biogeochemical model; Eutrophication; MERIS chlorophyll *a*; English Channel; Southern Bight of the North Sea; Model validation

* Corresponding author. Tel.: +32 2 773 21 00; fax: +32 2 770 69 72.
*E-mail addresses:* G.Lacroix@mumm.ac.be (G. Lacroix), K.Ruddick@mumm.ac.be (K. Ruddick), Y.Park@mumm.ac.be (Y. Park), ngypens@ulb.ac.be (N. Gypens), lancelot@ulb.ac.be (C. Lancelot).

0924-7963/$ - see front matter © 2006 Elsevier B.V. All rights reserved.
doi:10.1016/j.jmarsys.2006.01.010

## 1. Introduction

In order to manage effectively environmental problems, such as eutrophication, in the Southern Bight of the North Sea, it is necessary to establish a scientific understanding of cause–effect relationships between climatological and/or changing human activities and ecosystem response. The Belgian Coastal Zone (BCZ) in the Southern Bight of the North Sea is a highly dynamic system where waters of Atlantic origin are mixed with freshwater river inputs (Fig. 1). Eutrophication along the continental coastline of the Southern Bight of the North Sea leads to high-biomass algal blooms (mainly the Haptophycea *Phaeocystis globosa*) that spread over the entire area along a SW–NE axis in spring (Lancelot et al., 1987). Massive development of *Phaeocystis* colonies is regularly observed in the Southern Bight of the North Sea (e.g. Veldhuis et al., 1986; Lancelot et al., 1987; Riegman et al., 1992; Mills et al., 1994) and is sustained by freshwater inputs deficient in silicon but enriched in nitrogen and phosphorus (Rousseau et al., 2002b).

Due to the complexity of interactions between planktonic organisms, the link between nutrient inputs and coastal ecosystem function cannot be understood by simple correlation between events. Models describing ecosystem carbon and nutrient cycles as a function of environmental forcing are needed to help understand the dynamics of the ecosystem and assess the magnitude and extent of algal blooms and their response to changes in land-based nutrient inputs and climate (Lancelot et al., 2005). The biogeochemical MIRO model is specifically designed to study the link between anthropogenic nutrient loads and the magnitude and extent of diatom and *Phaeocystis* colony blooms in the Southern Bight of the North Sea. This model simulates carbon and nutrient cycles, resolving the complex biology of the bloom species and the coupling between the benthic and pelagic compartments that characterise this shallow coastal shelf sea ecosystem. To account for the impact of the hydrodynamics of the region, this biogeochemical model is coupled with a 3D hydrodynamic model developed for the region (Lacroix et al., 2004). Such a model can be used to investigate the relative effect of different factors on ecosystem dynamics by simulating scenarios. For example, the relative effect of a possible nitrogen and/or phosphorus river input reduction on diatoms/*Phaeocystis* distribution in the Southern Bight of the North Sea could be estimated by simulating scenarios of nutrient reduction.

However, particular attention must be paid to the validation of models and in an environmental management context the model should be shown to reproduce a series of observed annual cycles and their observed variability realistically (Radach and Moll, 2006) before being used for simulating future scenarios. The prediction capability of the model is thus tested through its ability to reproduce observations. In order to assess the model accuracy for simulation of the seasonal dynamics of nutrients and phytoplankton (diatoms and *Phaeocystis*), a high resolution time series of data is necessary. The data collected in the

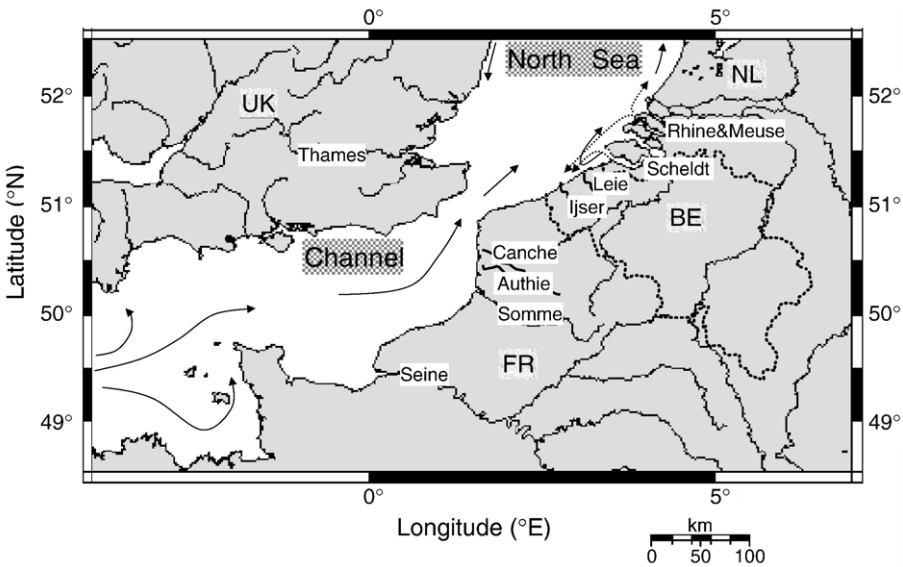


Fig. 1. Map of the Channel and the Southern Bight of the North Sea with schematic representation of the circulation (solid line) and dispersion (dotted line) (redrawn from Lacroix et al., 2004).

Southern Bight of the North Sea during the last decade (1991 to 2003), in particular at station 330 (51°26.00′N, 2°48.50′E) located in the centre of the Belgian coastal zone, is used for this purpose. In order to estimate the model accuracy for reproduction of the spatial distribution of monthly (or seasonal) nutrients and chlorophyll *a* concentration, data with sufficient space and time coverage are necessary. *In situ* measurements collected during cruises provide a high quality but very sparse data set in time and space for validation of biogeochemical results. They are therefore supplemented here by satellite chlorophyll *a* data from the MERIS sensor onboard ENVISAT (launched in March 2002).

Previous ecological model studies of the Southern North Sea and the English Channel show considerable diversity in the choice of biogeochemical state variables as well as the spatio-temporal resolution and coverage. In general, such diversity can be related to the dominant processes or species in the respective regions and/or the main model application and there is no generally accepted converged model. The ECOHAM model has been used to estimate annual primary production in the North Sea (Moll, 1997, 1998) using a phosphorus-based model, which has recently been updated to consider also a nitrogen-cycle (Skogen and Moll, 2005). An early two-layer model was used by Ménesguen and Hoch (1997) to study factors influencing primary production and eutrophication in the English Channel. More recently the 3D ELISE model has been used to study toxic dinoflagellate blooms in the Seine Bay (Cugier et al., 2005). The NORWECOM model (Skogen and Soiland, 1998) has been used, generally at coarser spatial resolution (e.g. 20 km) and with more focus on the Northern North Sea, to investigate, for example, primary production (Skogen et al., 1995) and impact of river discharge (Skogen et al., 1998). Variants of the ERSEM model (Baretta et al., 1995; Vichi et al., 2004) have been used to study, for example, long term eutrophication (Pätsch and Radach, 1997) and nutrient cycling (Allen et al., 2001) in the North Sea. Delhez (1998) characterises differences in primary production according to stratification in the North Sea. Luyten et al. (1999) use the COHERENS model to estimate monthly-averaged primary production in the Southern North Sea and Eastern Channel. A detailed review of these and other North Sea model studies is provided by Moll and Radach (2003). A general difference between MIRO&CO-3D and these other models, with the exception of ERSEM, is the much larger number of pelagic state variables and related processes and parameters used in MIRO (Lancelot et al., 2005). A second peculiarity of MIRO is the explicit description of the *Phaeocystis* dynamics and the experimental determination of most phytoplankton-related parameters. Conceptually, the MIRO model is thus best adapted to the study of *Phaeocystis*-dominated eutrophied ecosystems and the explicit consideration of all nutrients (phosphorus, nitrogen and silica) allows to investigate the response of the system to any shifts in nutrient loads as a result of mitigation.

The objective of this paper is to assess the ability of the MIRO&CO-3D model to reproduce the seasonal dynamics and the spatial distribution of nutrients and phytoplankton in Belgian waters. In the following section, the MIRO&CO-3D model will be presented and details of its implementation will be given. Then, details about the data set used for validation and the MERIS chlorophyll *a* images will be given. Finally, the model results and their validation with *in situ* data and MERIS chlorophyll *a* images will be presented and discussed.

## 2. Model description

The 3D hydrodynamical model of Lacroix et al. (2004) has been coupled with the biogeochemical MIRO model (Lancelot et al., 2005) to simulate the transport and seasonal dynamics of inorganic and organic carbon, nutrients, phytoplankton, bacterioplankton and zooplankton.

### 2.1. Hydrodynamical model

The 3D hydrodynamic model solves the continuity, momentum, heat and salinity transport equations on a staggered Cartesian, sigma coordinate grid with an explicit mode-splitting treatment of the barotropic and baroclinic modes. Advection of scalar quantities is discretised by a direction-split Total Variation Diminishing (TVD) scheme. Vertical diffusion is modelled using an evolution equation for turbulent kinetic energy and a quasi-parabolic vertical profile for turbulence macro-length scale. Minimal vertical diffusion and viscosity coefficients of $10^{-6}$ $m^2$ $s^{-1}$ are used. Horizontal diffusion is not considered explicitly, but the process of horizontal diffusion arising from the combination of horizontal advection with vertical diffusion is resolved. Advection of momentum is treated with a first order upwind scheme. Full details of all these methods as well as the original references can be found in Ruddick (1995) and Luyten et al. (1999).

### 2.2. Biogeochemical model. From MIRO to MIRO&CO-3D

The biogeochemical MIRO model includes thirty-two state variables and twenty-eight processes linking them

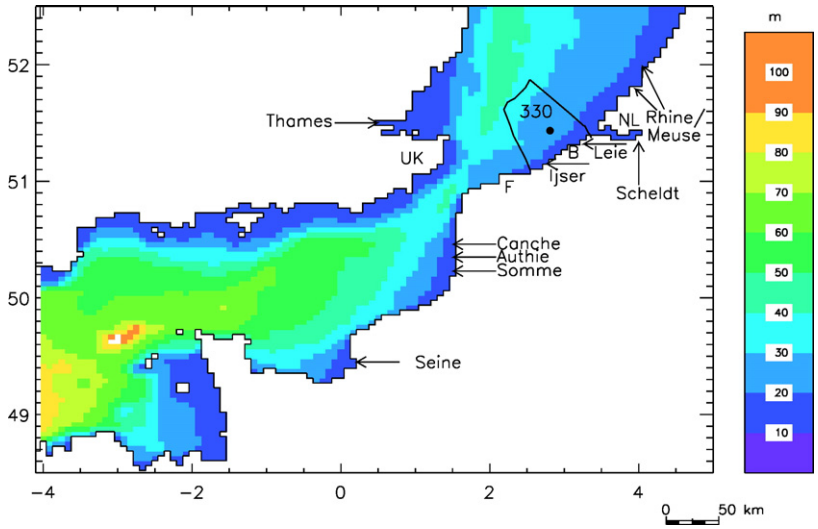


Fig. 2. Bathymetry (in m) of the Southern Bight of the North Sea and Channel model. The Belgian EEZ is delimited by the black line. The black dot denotes the station 330 of the Belgian water quality monitoring network used to present the results of Figs. 3, 4 and 5. The model domain is a 109 by 97 horizontal grid with resolution of 5′ longitude by 2.5′ latitude. Each pixel corresponds to one grid cell. River discharges are shown by red arrows.

were selected as important from knowledge of the structure and functioning of *Phaeocystis*-dominated ecosystems. The model results from the integration of 4 modules (phytoplankton, zooplankton, microbial loop and benthic diagenesis) describing: (i) the dynamics of phytoplankton [diatoms (DA), autotrophic nanoflagellates (NF) and *Phaeocystis* colonies (OP)], (ii) zooplankton [microzooplankton (MZ) and copepods (CP)], (iii) bacteria (BC) and dissolved (DOM) and particulate (POM) organic matter degradation and (iv) nutrient [nitrate ($NO_3$), ammonium ($NH_4$), phosphate ($PO_4$) and dissolved silica (DSi)] regeneration in the water column and the sediment. *Phaeocystis* free-living cells are included in NF, while *Phaeocystis* colonies are described by the sum of 2 state variables: colonial cells (OPC) and the polysaccharide matrix (OPM) in which the cells are embedded and which serves as a reserve of energy. Phytoplankton growth is described according to the AQUAPHY model of Lancelot et al. (1991), which considers 3 intracellular pools: monomers (S); reserve material (R, [OPM]); functional and structural metabolites (F). The degradation of organic matter by planktonic bacteria was described according to the HSB (High polymers, Small substrates and Bacteria) model of Billen and Servais (1989), considering 2 classes of biodegradability for DOM (DC1, DN1, DP1 and DC2, DN2, DP2) and POM (PC1, PN1, PP1 and PC2, PN2, PP2). The hydrolysis of these polymers produces dissolved monomers (BSC, BSN) that can be taken up by bacteria. Benthic organic matter degradation and nutrient (N, P, Si) recycling were calculated by the algorithms developed by Lancelot and Billen (1985) and Billen et al. (1989). A full description of the modules and a schematic representation of the MIRO model can be found in Lancelot et al. (2005). State variables, processes and conservation equations are detailed in Lancelot et al. (2005, Appendices available at www.int-res.com/journals/suppl/appendix_lancelot.pdf). The model has been implemented in a 3-box representation corresponding to the Belgian coastal zone (BCZ), the French coastal zone (FCZ) and the Western Channel (WCH) and has been validated by comparison between simulations and data collected in the different boxes (for details see Lancelot et al., 2005).

MIRO has been implemented in 3D with the following modifications to account for improvements in the representation of light-related processes and adaptations necessitated by a better representation of the physics.

In the 0D model, the PAR (Photosynthetically Active Radiation) attenuation is function of a box-dependant light extinction due to clear water and particulate suspended matter and a variable extinction due to chlorophyll *a* self-shading. In the 3D version a model (KPARv1) gives PAR attenuation coefficient as function of: (i) non-algae particle concentration, (ii) chlorophyll *a* concentration computed by the model, (iii) coloured dissolved organic matter (CDOM) absorption at 443 nm estimated from salinity computed by the model and (iv) depth. The non-algae particle concentration is estimated from total suspended matter (TSM) minus a fraction (function of the simulated chlorophyll *a* concentration) representing the algae contribution. A TSM seasonal

Table 1
Data sources for river flow rates

| River | Frequency | Data source |
|---|---|---|
| Scheldt (Schaar van Ouden Doel) | 10-day | Data collected by RIZA (Rijksinstituut voor Integraal Zoetwaterbeheer en Afvalwaterbehandeling, Ministerie van Verkeer en Waterstaat) and archived into the central data base DONAR were downloaded from the waterbase web site http://www.waterbase.nl. |
| Leie (Zeebrugge), Ijser (Nieuwpoort) | 10-day | River flow estimated from Scheldt river flow and respective contribution compared to Scheldt from YZEUT report (Rousseau et al., 2002a) |
| Rhine/Meuse (Hoek van Holland and Haringvlietsluis) | Daily | Data collected by RIZA (Rijksinstituut voor Integraal Zoetwaterbeheer en Afvalwaterbehandeling, Ministerie van Verkeer en Waterstaat) and archived into the central data base DONAR were downloaded from the waterbase web site http://www.waterbase.nl |
| Seine (Poses) | Daily | Data collected by the Cellule anti-pollution DDE (Service de Navigation de la Seine de Rouen SNS) and downloaded from the web site http://seine-aval.crihan.fr/rubriques/estuaire_seine/rubriques/donnees_brutes/debits/debits-Seine.htm |
| Somme (Abbeville), Authie (Quend), Canche (Brimeux) | Daily | Data downloaded from the Artois-Picardie Water Agency web site http://www.eau-artois-picardie.fr/bassin/index.htm |
| Thames (Kingston) | Daily | Data collected under the responsibility of the UK Environment Agency and downloaded from the NRFA web site (National River Flow Archive, http://www.nwl.ac.uk/ih/nrfa/webdata) |

climatology, spatially averaged to match the model grid cells, has been built from 1997–2002 SeaWiFS images using the algorithm of Nechad et al. (2003). Between seasons, TSM is temporally interpolated. Not enough TSM satellites images are available to allow an increase of the temporal resolution and to account for the interannual variability. The KPARv1 model is based on a look up table which has been generated using typical specific inherent optical properties for North Sea water in a similar way to the model of Buiteveld (1995). This provides a much better representation of spatial variability of light attenuation for the whole range of conditions from the deep and relatively clear water of the central English Channel to the turbid coastal waters of the Belgian and Dutch coasts. The maximum for the light adaptation parameter has been changed (Ekmax = 50 μmol $m^{-2}$ $s^{-1}$ in place of 65 μmol $m^{-2}$ $s^{-1}$ in the 0D model (Lancelot et al., 2005)).

The difference in nutrient inputs from rivers, injected directly to coastal waters in the 0D model but advected from the estuaries by modelled currents in the 3D model, gives greater nutrient limitation and hence lysis in the 3D model. The minimum specific rate of diatom cellular autolysis has thus been adapted (klysDA min = 0.001 $h^{-1}$ in place of 0.0016 $h^{-1}$ in the 0D model).

### 2.3. MIRO&CO-3D implementation

The coupled MIRO&CO-3D model has been set up for the region between 48.5°N (4°W) and 52.5°N (5°E) with the bathymetry shown in Fig. 2 using a 109 by 97 horizontal grid with resolution 5′ longitude (approx.

Table 2
Data sources for river discharges of dissolved and particulate nutrients

| River | Frequency | Data source |
|---|---|---|
| Scheldt (Schaar van Ouden Doel) | (Bi)-monthly | RIKZ (Rijksinstituut voor Kust en Zee) concentrations downloaded from the DONAR waterbase (http://www.waterbase.nl) at Schaar van Ouden Doel and reduced to salinity 0 by linear regression |
| Leie (Zeebrugge), Ijser (Nieuwpoort) | (Bi)-monthly | Discharges estimated from Scheldt river discharges and respective contribution compared to Scheldt from YZEUT report (Rousseau et al., 2002a) and specified as concentrations. |
| Rhine/Meuse (Maassluis and Haringvlietsluis) | (Bi)-monthly | RIKZ (Rijksinstituut voor Kust en Zee) concentrations downloaded from the DONAR waterbase (http://www.waterbase.nl) |
| Seine (Caudebec) | Bi-monthly | Concentrations measured by the DDE-SNS Rouen and received from the RNB (Réseau National des Bassins) (Ficht, 2003. pers. comm.). |
| Somme (Cambron), Authie (Quend), Canche (Beutin) | Monthly | Concentrations downloaded from the Artois Picardie Water Agency (RNB) web site (http://www.eau-artois-picardie.fr/bassin/index.htm). |
| Thames (Teddington) | (Bi)-monthly | Dissolved nutrient discharges are specified as concentrations coming from the UK Environment Agency measurements (Lewis, 2003. pers. comm.). Organic nutrients are specified as concentrations derived from the North Sea Task Force guidance document (Rijkswaterstaat, 1992) and corresponding to the NSTF "reference year" of 1985 |

5.6 km) by 2.5′ latitude (approx. 4.6 km) and with 5 vertical sigma coordinate layers. The model is run with mode-splitting time steps of 60 s and 900 s respectively for 2D and 3D calculations.

At the Western ("Channel", 4°W) and Northern ("Central North Sea", 52.5°N) open sea boundaries the time series of cross-boundary transport (vertically integrated current) and surface elevation are applied using data from a 2D model of the North Sea continental shelf also based on the COHERENS software (Luyten et al., 1999). This 2D model is forced by 6-hourly wind and atmospheric pressure fields from the analysed/forecast data of the UK Meteorological Office, and transfers this meteorological forcing in turn to the COHERENS-3D model. The wind forcing is spatially variable on a grid with resolution varying from 1.25° to 5° in longitude and 1.25° to 2.5° in latitude according to available data. At the two open sea boundaries the vertical current structure is determined by imposing the condition of zero normal derivative of the deviation of current from the vertically-averaged horizontal current (Deleersnijder et al., 1989), while at river boundaries a condition of zero vertical gradient of current is applied. River flow rates have been collected from various sources or estimated (Table 1). The position of the rivers is shown in Fig. 2.

For temperature, zero flux is assumed at the sea bottom. The spatially variable temperature imposed at the surface is derived from the weekly sea surface gridded temperature (on a grid of 20 km × 20 km) obtained from the BSH (Bundesamt fuer Seeschiffahrt und Hydrographie) (Loewe, 2003). For periods without SST data (1991–1995), a weekly climatological SST (computed from 1996–2000 BSH data) is imposed. At the open sea boundaries and river boundaries, a zero horizontal cross boundary gradient of temperature is specified.

For salinity, a zero flux is assumed at the sea bottom and sea surface boundaries. The incoming salinity at the river boundaries is set to zero. At the open sea boundaries, no boundary condition is required when the current is directed out of the domain. For inflow periods, the salinity at the Channel boundary is specified as 35 psu and corresponds to an average from ICES data. At the Central North Sea boundary a salinity of 34.45 psu is specified west of 4°E, based on the Damm (1989) climatology, while east of this longitude a zero horizontal cross boundary gradient of salinity is specified to allow realistic formation of the Rhine plume and associated Dutch coastal current.

At the Channel and Central North Sea open sea boundaries a zero horizontal cross boundary gradient is specified for biological state variables. At the Channel and Central North Sea (West of 4°E) open sea boundary nutrient concentrations are specified as concentrations derived from climatological databases compiled by the European Union NOWESP and ERSEM projects (Radach and Lenhart, 1995) and from ICES data, while East of this longitude a zero horizontal cross boundary gradient of nutrients is specified.

Dissolved ($NO_3$, $NH_4$, $PO_4$, Si) and particulate (Norg, Porg) nutrient discharges from the rivers have been collected from various sources (Table 2).

Initial conditions for salinity and for biological state variables, except nutrients, are assumed horizontally and vertically homogeneous. The initial distribution of nutrients over the domain has been reconstructed making use of various databases: BMDC (Belgian Marine Data Centre, http://www.mumm.ac.be/datacentre/), DONAR waterbase (http://www.waterbase.nl), ICES (International Council for the Exploration of the Sea, http://www.ices.dk). To reduce the sensitivity of results to these initial conditions a two year spin-up MIRO&CO-3D simulation was run for the period January 1991–December 1992 with the aforementioned initial and open boundary conditions and forcing. A baseline simulation was then carried out for the period January 1993–December 2003. A sensitivity study has shown insensitivity to perturbation of the biological initial conditions after two years of simulation.

## 3. Validation data

### 3.1. Station 330 time series

Time series at the reference station 330 (see Fig. 2) is used for the validation of nutrients and phytoplankton seasonal dynamics. A high resolution time series with several state variables is available, since station 330 was set up for monitoring the seasonal and interannual variations of algal blooms and related parameters. Data include temperature, chlorophyll *a*, nutrients, DOC, phytoplankton, bacteria, and micro- and mesozooplankton sampled at weekly or 2-weekly intervals between 1989 and 2000 (Lancelot et al., 2004). For this comparison, the model chlorophyll *a* was calculated by adding the simulated DAF, NFF and OPF and using a Chlorophyll *a*:C factor of 0.04 (mg:mg; after Lancelot-Van Beveren, 1980).

### 3.2. MERIS-derived surface chlorophyll a images

*In situ* measurements collected during cruises provide a data set for validation of biogeochemical results that is of high quality but very sparse in time and space. Seaborne monitoring of a network of points in Belgian waters made about every two months can miss entirely the spring phytoplankton bloom on some years (Ruddick et al.,

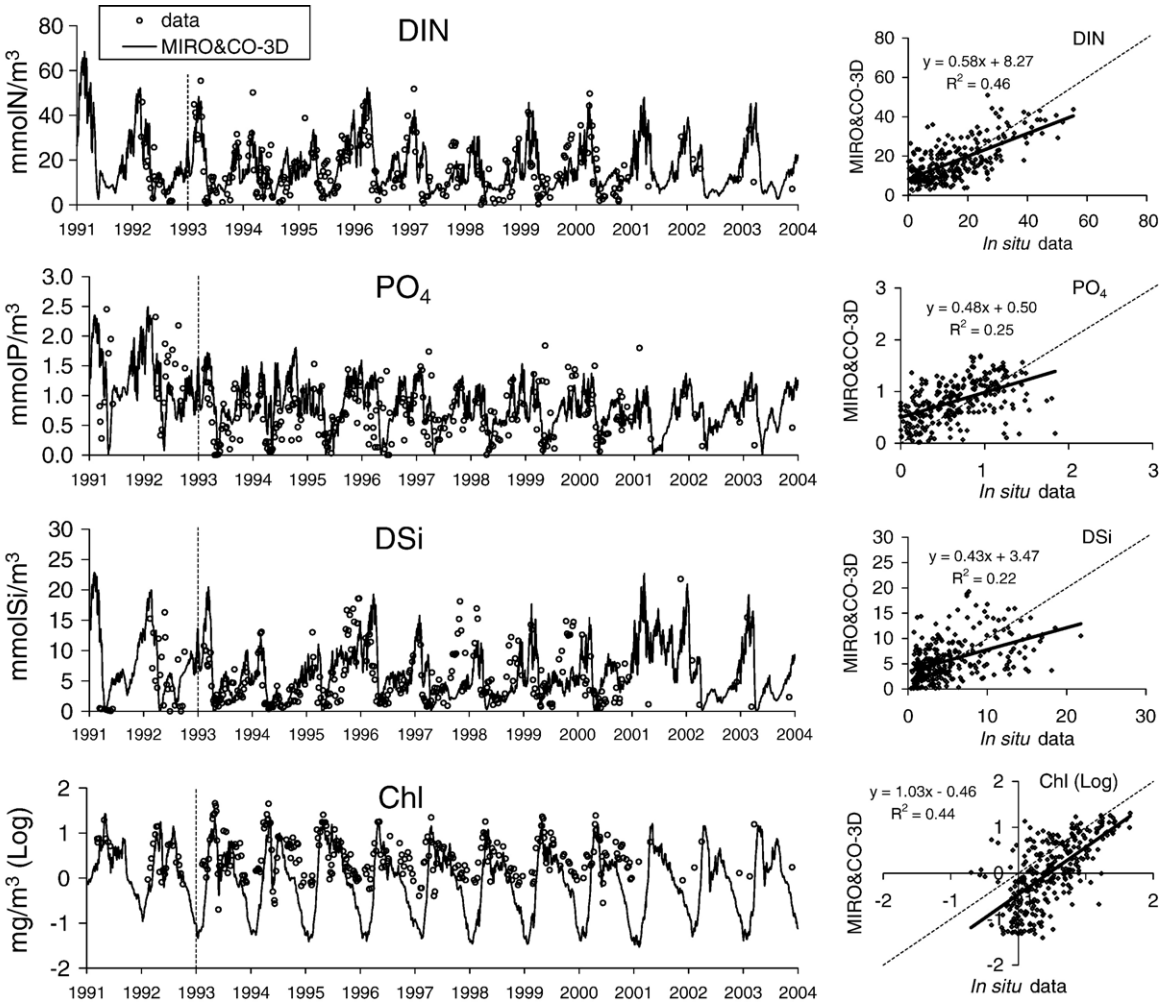


Fig. 3. Left panel: Time series of MIRO&CO-3D model results in the Belgian EEZ for the station 330 (51° 26.00′N, 2° 48.50′E) (solid line). Time series of *in situ* data (1991–1999: Lancelot et al., 2004; 2000–2003: BMDC) for the station 330 (dots). The dashed vertical line delimits the 2-year spin up period. Right panel: Scatter plot of model results versus *in situ* data (1993–2003). The dashed line corresponds to model result: *in situ* data ratio of 1. From top to bottom: DIN, $PO_4$, DSi, chlorophyll *a* (log scale).

1999). Even weekly monitoring of a single station (e.g. station 330, Rousseau, 2000) might be insufficient to accurately estimate the interannual variability of the chlorophyll *a* maximum. Satellite imagery, therefore, represents a powerful additional source of data for model validation, providing far superior spatial coverage as well as reasonable temporal coverage (approximately daily during cloud-free periods). However, care is needed in the use and interpretation of satellite imagery especially in turbid coastal waters where problems of atmospheric correction and absorption from non-algae particles and coloured dissolved organic matter can degrade or render completely unusable chlorophyll *a* imagery. In the present study only data from the MERIS sensor has been used because of certain advantages of this sensor and the processing algorithms: the 709 nm band improves chlorophyll *a* detection in coastal waters (Gons et al., 2005) and the atmospheric correction (Moore et al., 1999) and chlorophyll *a* retrieval algorithm (Schiller and Doerffer, 1999) have been designed from the outset to cover coastal waters. However this does not prove the reliability of MERIS chlorophyll *a*, especially for case 2 waters. Therefore, considerable attention has been paid to automated quality assessment of MERIS products and a "product confidence" flag is provided for each pixel for each product denoting whether the data is suspect or acceptable. This allows masking of the less reliable data, which might have been shown as pretty but invalid pictures. Validation of the MERIS products for Belgian waters is reported by Park et al. (2003).

Table 3
Average *in situ* and simulated nutrients (mmol/m$^3$) and chlorophyll *a* (mg/m$^3$) concentration over the period 1993–2003

| | DIN ($N$=246) | $PO_4$ ($N$=263) | DSi ($N$=278) | Chl ($N$=288) |
|---|---|---|---|---|
| Model results | 17.57 | 0.82 | 5.76 | 3.03 |
| *In situ* data | 15.95 | 0.66 | 5.24 | 5.35 |
| *In situ* data standard deviation | 11.80 | 0.41 | 4.43 | 6.92 |
| −−data)/data)*100 | +10.16% | +24.66% | +9.92% | −43.36% |

Only model results corresponding to the same dates as observations have been considered for the mean.

It is difficult to use satellite chlorophyll *a* for validation of model-derived results for parameters such as timing and duration of the spring phytoplankton bloom or peak chlorophyll *a* concentration because of loss of data during cloudy periods. However, satellite chlorophyll *a* data is very well suited for validation of spatial maps of temporally-averaged model results for chlorophyll *a*, showing regions where the model may be performing less well.

Two algal pigment indices are provided as MERIS water products. The "algal1" product is computed using a ratio of water-leaving reflectances at blue and green bands (Morel, 1988) and represents chlorophyll *a* concentration for oceanic "case 1" waters where only phytoplankton and its degradation products affect the optical properties of water. The "algal2" product is designed to represent chlorophyll *a* concentration for case 2 waters, where other constituents such as inorganic sediments and coloured dissolved organic matter have significant impact on water colour. This product is calculated using a neural-network multiband spectral inversion technique (Schiller and Doerffer, 1999). In the present study the algal2 product was used for pixels for which the MERIS case2 water flag was set and the algal1 product was used for the remaining case 1 water pixels. Pixels for which the corresponding product confidence flag was raised were removed, thus excluding data contaminated by sun glint and clouds or other atmospheric correction problems and data for which chlorophyll *a* retrieval is considered as unreliable. Each MERIS image was spatially averaged to match the model grid cells. These daily images were then aggregated to give weekly binned images, which were also further processed to yield monthly images. The binned images include parameters such as mean, maximum, minimum, standard deviation and number of images used. MERIS data used here correspond to the spring 2003 archive reprocessing.

## 4. Model results and validation

### 4.1. Salinity

A preliminary step in the validation procedure of the biogeochemical model consists in validation of the hydrodynamics. For this the most relevant parameter is salinity, which is advected and diffused in a very similar way to most biogeochemical parameters, including nutrients in winter. A comparison between simulated and measured salinity in the Belgian waters has shown good agreement between model results and *in situ* data (Lacroix et al., 2004).

Table 4
Cost function (regional scale, time resolving for specific stations, according to OSPAR et al., 1998) for DIN, $PO_4$, DSi and chlorophyll *a* concentrations for the period 1993–2003 at different stations

| | Position | | | Cost function | | | |
|---|---|---|---|---|---|---|---|
| Station | Latitude (°N) | Longitude (°E) | Data source (details in Table 5) | DIN | $PO_4$ | DSi | Chl |
| 130 | 51.271 | 2.905 | BMDC | 0.56 | 0.49 | 0.59 | 0.31 |
| 230 | 51.308 | 2.850 | BMDC | 0.40 | 0.62 | 0.51 | 0.33 |
| 330 | 51.433 | 2.808 | ULB & BMDC | 0.28 | 0.54 | 0.72 | 0.35 |
| 435 | 51.581 | 2.790 | BMDC | 0.30 | 0.40 | 0.41 | 0.40 |
| 800 | 51.847 | 2.867 | BMDC | 0.36 | 0.59 | 0.38 | 0.45 |
| Goeree 6 km | 51.870 | 3.874 | RIKZ | 0.74 | 0.78 | 1.07 | 0.38 |
| Noordwijk 2 km | 52.261 | 4.406 | RIKZ | 0.19 | 0.19 | 0.25 | 0.35 |
| Noordwijk 10 km | 52.302 | 4.303 | RIKZ | 0.30 | 0.58 | 0.58 | 0.33 |
| Noordwijk 20 km | 52.342 | 4.175 | RIKZ | 0.36 | 0.68 | 0.76 | 0.30 |
| Walcheren 2 km | 51.549 | 3.411 | RIKZ | 0.19 | 0.23 | 0.29 | 0.42 |
| Walcheren 20 km | 51.659 | 3.221 | RIKZ | 0.31 | 0.32 | 0.34 | 0.61 |
| Walcheren 70 km | 51.957 | 2.679 | RIKZ | 0.56 | 0.77 | 0.56 | 0.70 |
| Dunkerke 4 | 51.152 | 2.252 | SRN | 0.42 | 0.35 | 0.50 | 0.84 |
| Boulogne 3 | 50.749 | 1.451 | SRN | 0.26 | 0.34 | 0.63 | 0.50 |
| Somme Mer 1 and 2 | 50.227 | 1.454 | SRN | 0.20 | 0.22 | 0.36 | 0.61 |

### 4.2. Time series of nutrients and chlorophyll a concentration

To estimate the reliability of the model, a comparison between model results and *in situ* measurements (Lancelot et al., 2004; BMDC data) for nutrients and chlorophyll *a* concentrations at station 330 is presented in Fig. 3. To visualize systematic differences between model results and data, a scatter plot showing simulated versus *in situ* measurements (Fig. 3, right panel) is presented in addition to the 1991–2003 time series plot of model results and data (Fig. 3, left panel). To allow an objective analysis a linear regression is produced (slope and $R^2$ in the figure) and the root mean square error (RMSE) has been estimated. For the chlorophyll *a*, plots are log–log and the regression is carried out in log–log space. Comparison between model results and *in situ* measurements shows that the model tends to underestimate nutrients (DIN, $PO_4$ and DSi) at highest concentrations and overestimate at low concentrations (Fig. 3, right panel). The simulated chlorophyll *a* seems systematically underestimated (Fig. 3, left panel). Examination of the scatter plot with simulated versus *in situ* chlorophyll *a* concentration (Fig. 3, right panel) confirms the general tendency of the model to underestimate the chlorophyll *a* concentration and shows a systematic underestimation at high (>10 mg/m$^3$) chlorophyll *a* concentrations. For some lower values, the model overestimates the chlorophyll *a* concentration. The correlation between model results and data is better for DIN ($R^2$=0.46) and chlorophyll *a* ($R^2$=0.44) than for $PO_4$ ($R^2$=0.25) and DSi ($R^2$=0.22). The RMSE is respectively equal to 9.05 mmolN/m$^3$, 0.43 mmolP/m$^3$, 4.38 mmolSi/m$^3$ and 5.43 mgChl/m$^3$ for DIN, $PO_4$, DSi and chlorophyll *a*. To provide an objective quantification of model performance, a 1993–2003 average (arithmetic) of *in situ* and simulated nutrients and chlorophyll *a* concentrations can be found in Table 3. It appears that the nutrient concentration is on average overestimated by the model while chlorophyll *a* concentration is underestimated. The relative difference between simulated and *in situ* mean concentration [(simulated mean concentration minus *in situ* mean concentration)/*in situ* mean concentration * 100] is respectively equal to 10% for DIN, 25% for $PO_4$, 10% for DSi and −43% for chlorophyll *a*.

An objective way to estimate the reliability of the model consisting to compute the cost function to measure the goodness of fit between the model and measurements (OSPAR et al., 1998; Radach and Moll, 2006). The cost function is a mathematical function which provides a useful means of comparing data from different sources, e.g. model results and observations. The cost function gives a non-dimensional number which is indicative of the goodness of fit between the two data sets. Here, the cost function proposed in OSPAR et al. (1998) to validate models at a regional scale, time resolving for specific stations has been applied. A full description of the way to

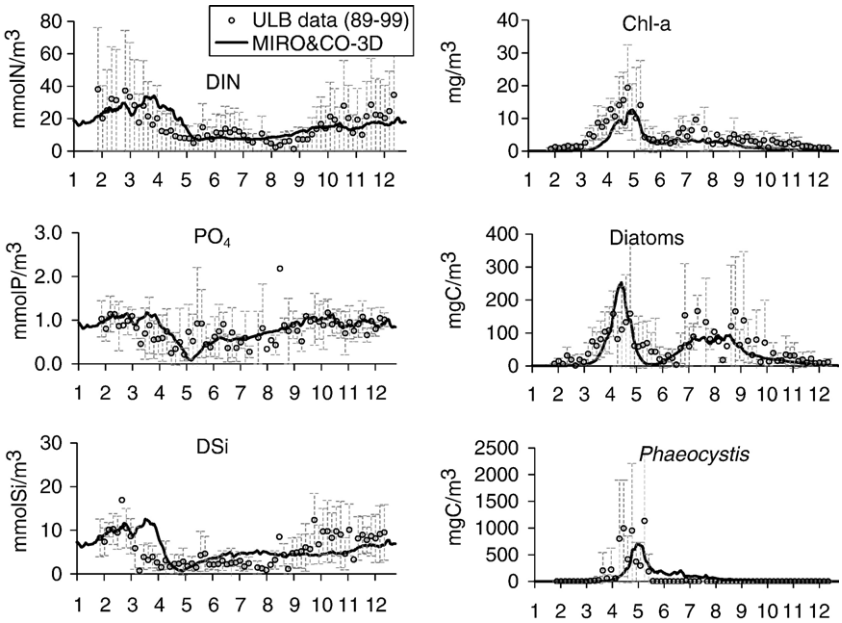


Fig. 4. Seasonal evolution of MIRO&CO-3D model results in the Belgian EEZ for the station 330 (solid line). 5-day averaged (+/− standard deviation) *in situ* data (1989–1999: Lancelot et al., 2004) for the station 330 (dots). On the left: nutrients (DIN, $PO_4$, DSi). On the right: phytoplankton biomass (chlorophyll *a*, diatoms and *Phaeocystis*).

compute this cost function can be found in OSPAR et al. (1998) and Radach and Moll (2006). The cost function for DIN, $PO_4$, DSi and chlorophyll *a* concentrations has been computed for the period 1993–2003 at different stations. The position of the stations, data sources and the cost functions can be found in Table 4. In Radach and Moll (2006), the authors propose an interpretation of the values of the cost functions adapted from the OSPAR et al. (1998) rating. Model results are respectively very good, good, reasonable and poor for cost function between 0 and 1, 1 and 2, 2 and 3 and finally, higher than 3. According to this classification the MIRO&CO-3D results are all very good except for the DSi results at Goeree 6 km. This station is situated very close to the Rhine/Meuse input in

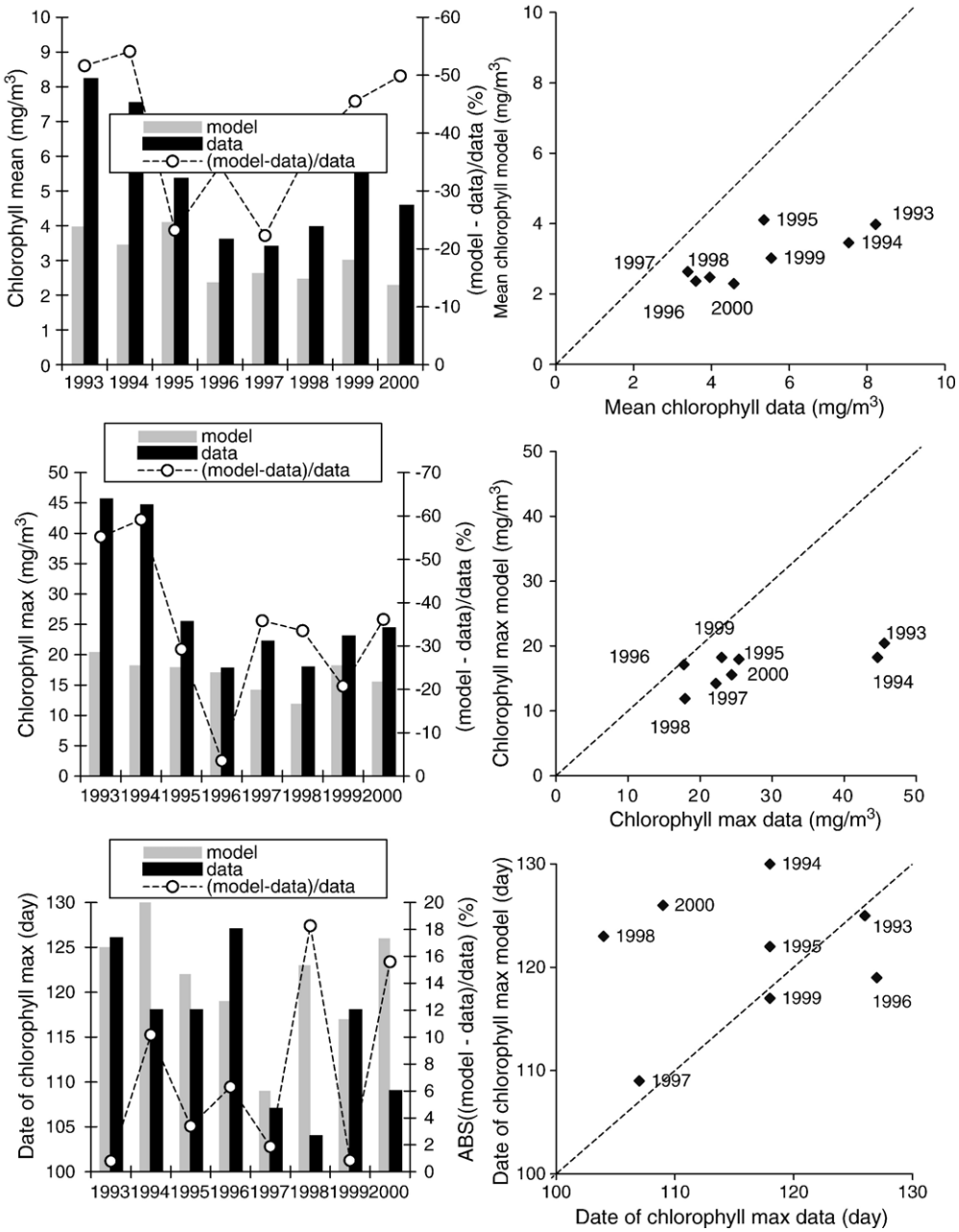


Fig. 5. Left panel: Annual (1993–2000) model results (grey bars) and *in situ* data (black bars) and superimposed relative difference (circles) between them. Station 330 shown in Fig. 2. From top to bottom: Annual mean chlorophyll *a* (mg/m$^3$), chlorophyll *a* maximum (mg/m$^3$) and date of the chlorophyll *a* maximum (day). Right panel: scatter plot of the same values.

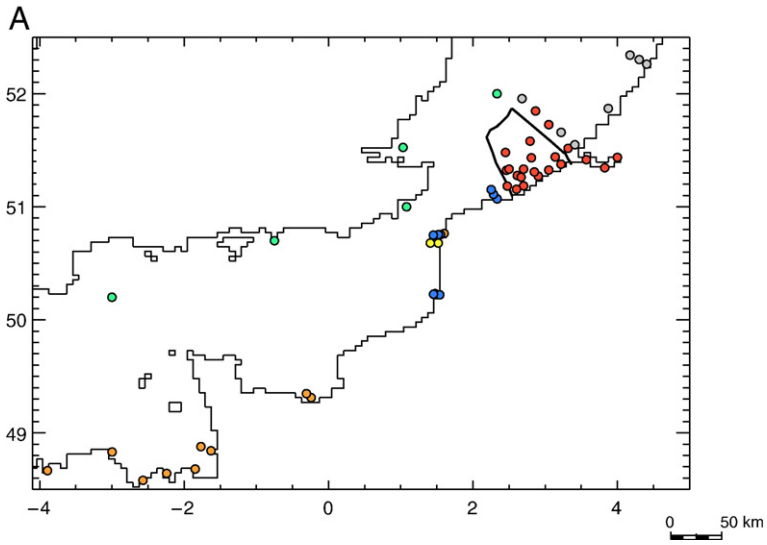


Fig. 6. A. Position of the stations used for the model validation. Different colours correspond to the data sources: BMDC (red), RIKZ (grey), SOMLIT (yellow), REPHY (chlorophyll: orange), SRN (blue), CEFAS (nutrient: green). Information about the data sources can been found in Table 5. B. 1993–2003 averaged surface winter (resp. spring) nutrient (resp. chlorophyll *a*) concentrations obtained with MIRO&CO-3D model. Superimposed coloured circles correspond to the *in situ* data averaged over the same season. Colour scale is the same for model results and data. C. Relative difference (%) between model results and *in situ* data shown in Fig. 6B for stations shown in Fig. 6A. Red: >50%, orange: [25%, 50%], yellow: [0%, 25%], green: [−25%, 0%], light blue: [−50%, −25%], dark blue: < −50%.

the model. While the thresholds chosen to define "good" results remain arbitrary, the cost function approach is particularly effective for comparing the results of different models when cost functions are available for the same stations. Cost functions (on regional scale, time resolving, specific stations) for the station Noordwijk 10 km are given for three models in OSPAR et al. (1998): DYMONNS, DCM-NZB and CSM-NZB and for DIN and chlorophyll *a* concentration. For DYMONNS model, the cost functions are respectively equal to 1.18 and 0.27 for DIN and chlorophyll *a*. For DCM-NZB, the cost functions are respectively equal to 0.84 and 0.47 for DIN and chlorophyll *a*. For CSM-NZB, the cost functions are respectively equal to 1.36 and 0.66 for DIN and chlorophyll *a*. Except for DIN, the results of these models are also classified as very good.

The mean seasonal evolution (corresponding to an average of seasonal evolution for each year between 1993 and 2003) of simulated nutrients and chlorophyll *a* concentration and of diatoms and *Phaeocystis* is shown in Fig. 4. The comparison with 5-day averaged *in situ* data (1989–1999) allows a more precise assessment of the model ability to simulate the timing and magnitude of the diatom and *Phaeocystis* blooms and the seasonal dynamics in general. The annual cycles of phosphate and DIN are well reproduced (model results inside the observation variability) by the model. Nevertheless the simulated winter DIN concentration is underestimated and the spring concentration decreases too slowly. Except at the beginning of the spring bloom, the simulated chlorophyll *a* concentration is within the variability of measurements. Nevertheless, the simulated chlorophyll *a* maximum is underestimated presumably as a direct result of underestimation of the *Phaeocystis* peak compared to the observations. The timing of the diatom and *Phaeocystis* blooms is simulated with a slight delay compared to the observations. The most obvious qualitative difference between model results and measurements relates to the time series for dissolved silica where model results lie well outside the variability of measurements for April, suggesting imperfections in the representation of the silica cycle and in particular the early spring diatoms. Analysis of some model results (not shown) seems to indicate that the low simulated chlorophyll *a* concentration could result from a combined effect of an overestimation of the phytoplankton losses and nutrient limitation. Further simulations made with a decrease of phytoplankton losses (decrease of minimum specific rate of cellular autolysis for diatoms and/or *Phaeocystis*) have lead to higher maxima of chlorophyll *a*.

For chlorophyll *a*, a year by year comparison between model results and *in situ* data for annual mean chlorophyll *a* and chlorophyll *a* maximum (concentration and date) is shown in Fig. 5 (left panel). In Fig. 5 (right panel) the

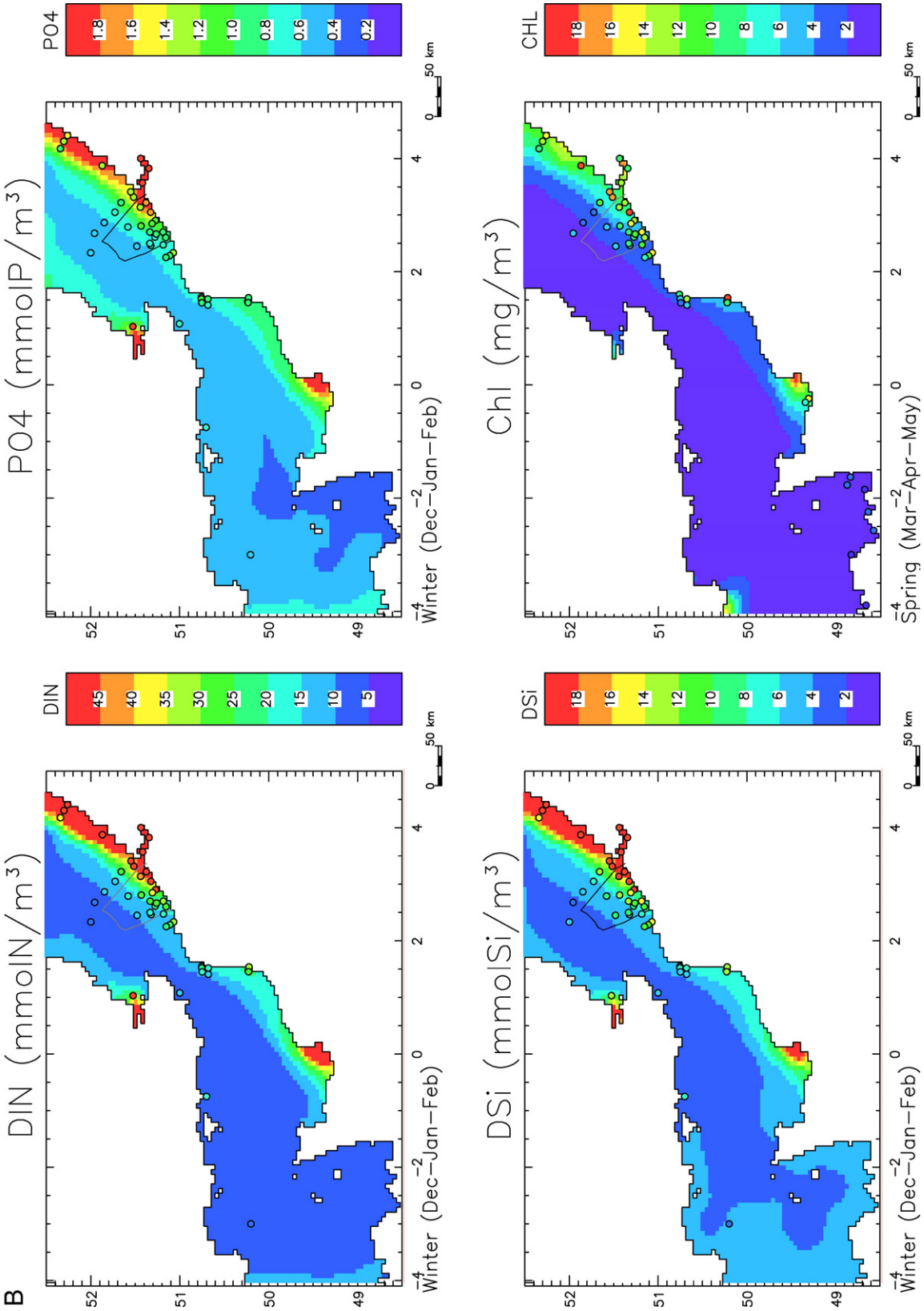


Fig. 6 (*continued*).

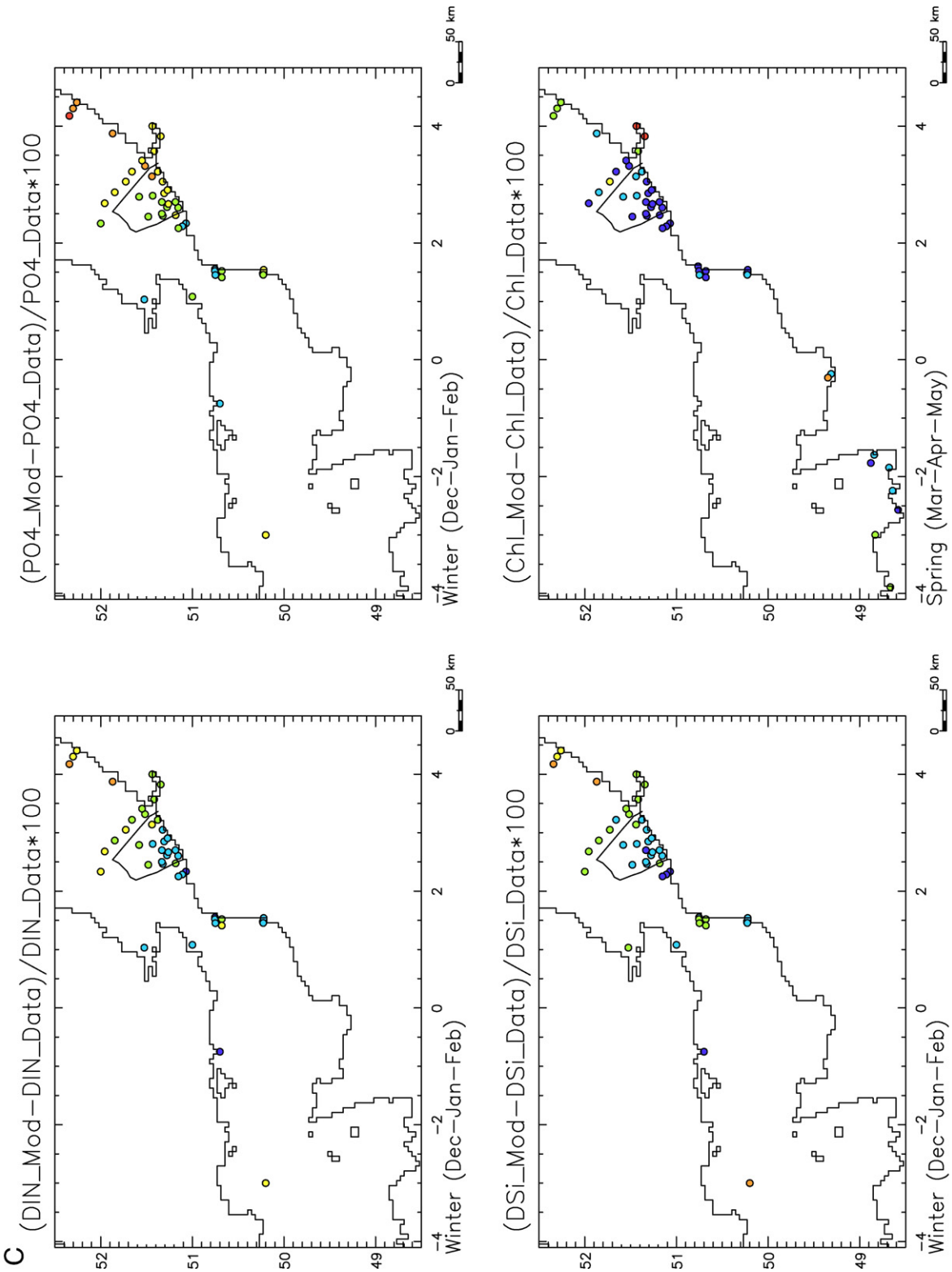


Fig. 6 (*continued*).

Table 5
Data sets used for validation of model results for seasonal surface nutrients and chlorophyll *a* concentration

| Data set name | Parameters | Periods | Source |
|---|---|---|---|
| BMDC | Nutrients and chlorophyll *a* concentration | 1993–2003 | Belgian Marine Data Centre. Data downloaded from the BMDC database http://www.mumm.ac.be/datacentre/ |
| RIKZ | Nutrients and chlorophyll *a* concentration | 1993–2002 | Ministry of Transport Public Works and Water Management, National Institute for Coastal and Marine Management / RIKZ, Department of Monitoring and Assessment. Data downloaded from the DONAR database http://www.waterbase.nl. |
| SOMLIT | Nutrients and chlorophyll *a* concentration | 1998–2003 | Data provided by "Service d'Observation en Milieu Littoral (SOMLIT), INSU-CNRS, WIMEREUX" |
| REPHY | Chlorophyll *a* concentration | 1990–2003 | Réseau de Surveillance du Phytoplancton et des Phycotoxines (REPHY), IFREMER. Data downloaded from IFREMER web site http://www.ifremer.fr/envlit/ |
| SRN | Nutrients and chlorophyll *a* concentration | 1993–2003 | "Suivi Régional des Nutriments" (SRN) for the coastal region Nord Pas de Calais Picardie organised by Ifremer and l'Agence de l'Eau Artois Picardie in 1992. For data after 2002, SRN Network (collaboration Ifremer/Ministère de l'Ecologie et du Développement Durable). |
| CEFAS | Nutrients concentration | 1991–2001 (seasonal average) | National Marine Monitoring Programme (NMMP), CEFAS. Data extracted from iSEA-interactive Spatial Explorer and Administrator (http://www.cefas.co.uk/isea/) |

same values are presented on scatter plots. Years 2001 to 2003 have not been considered because of the very low number of *in situ* data. Examination of these figures shows that both annual mean and maximum chlorophyll *a* concentration are underestimated by the model each year. For the years 1993 and 1994 values are less accurate with a relative difference between model and observations higher than 50% for both mean and maximum chlorophyll *a* concentrations. The annual mean (resp. max) chlorophyll *a* concentration is underestimated by a factor between 25% and 50% for the years 1996, 1998, 1999 and 2000 (resp. 1995, 1997, 1998 and 2000). A lower underestimation, less than 25%, is found for the annual mean (resp. max) chlorophyll *a* in 1995 and 1997 (resp. 1996 and 1999). The timing of the chlorophyll *a* maximum is well simulated (difference between simulated and observed maximum of chlorophyll *a* less than the average sampling frequency, that is 10 days) for the years 1993, 1995, 1996, 1997 and 1999 for which the difference between simulated and observed date of chlorophyll *a* maximum is respectively equal to −1 day, +4 days, −8 days, +2 days, −1 day.

### 4.3. Seasonal average (1993–2003) of surface nutrients and chlorophyll a concentration

A comparison between simulated and measured winter (Dec–Jan–Feb average) surface nutrients and spring (Mar–Apr–May average) surface chlorophyll *a* concentration is shown in Fig. 6. Stations for which measurements are used for validation have been selected according to the number of available data (at least one per month) within the period 1993–2003 (Fig. 6A). The data sources are given in Table 5. Contour plots of 1993–2003 averaged surface winter (Dec–Jan–Feb) nutrients and spring (Mar–Apr–May) chlorophyll *a* concentrations calculated by the model are shown in Fig. 6B. In this figure, *in situ* data averaged over the same season are superimposed as coloured circles. In order to have an idea of the model reliability to reproduce the correct spatial distribution for the considered seasons, the Fig. 6C shows the relative difference between model results and *in situ* measurements. Table 6 gives for each nutrient and for chlorophyll *a* concentration, the percentage of stations for which the

Table 6
Percentage of stations for which the relative difference between model results (winter nutrients and spring chlorophyll *a*) and *in situ* measurements are within different ranges of over-underestimation for the period 1993–2003

| Relative difference between model and *in situ* data | Winter DIN (93-03) $N$=45 | Winter $PO_4$ (93-03) $N$=45 | Winter DSi (93-03) $N$=45 | Spring Chl (93-03) $N$=51 |
|---|---|---|---|---|
| >75% | 0% | 0% | 0% | 2% |
| [50%, 75%] | 0% | 2% | 0% | 2% |
| [25%, 50%] | 4% | 11% | 7% | 2% |
| [0, 25%] | 18% | 36% | 4% | 2% |
| [−25%, 0%] | 27% | 36% | 36% | 12% |
| [−50%,−25%] | 44% | 15% | 40% | 23% |
| [−75%,−50%] | 7% | 0% | 13% | 51% |
| < −75% | 0% | 0% | 0% | 6% |

$N$ is the number of stations.

relative difference between model results and data are within different ranges of over-underestimation. From this table, it appears that, for the seasons considered, the model tends to underestimate *in situ* concentrations in general. Respectively for 78%, 51%, 89% and 92% of stations the model underestimates DIN, $PO_4$, DSi and chlorophyll *a* concentrations and for 22%, 49%, 11% and 8% of the stations, the model gives an overestimation. Examination of Fig. 6c shows that, significant overestimation (>50%) is only found for chlorophyll *a* at two stations (Scheldt estuary) and for $PO_4$ at one station very close to the northern boundary. Simulated DIN, $PO_4$ and DSi show moderate ([25%, 50%]) overestimation close to the Rhine/Meuse mouth and the Scheldt estuary (for $PO_4$ only). Significant underestimation (< −50%) is found mainly for chlorophyll *a* (29 stations), then for DSi (6 stations) and for DIN (3 stations). $PO_4$ seems better simulated than other nutrients. For respectively 45% (DIN), 72% ($PO_4$) and 40% (DSi) of the stations, the model gives a good estimation (relative difference between model results and *in situ* measurements is within the range [−25%, 25%]).

### 4.4. 2003 surface chlorophyll a

The validation of the previous sections is limited by use of only a few stations with non-uniform spatial coverage and very limited temporal coverage. The validation exercise is therefore extended to the whole domain and with better temporal coverage by using surface chlorophyll *a* data derived from MERIS.

The monthly (from March to July) mean surface chlorophyll *a* concentration from MERIS for the year 2003 is shown in Fig. 7 (left panel). For the purpose of model validation, satellite-derived chlorophyll *a* concentration has been averaged horizontally over the model grid cells. The corresponding monthly mean surface (top σ-layer) chlorophyll *a* concentration obtained by the model and the relative difference between simulated and MERIS chlorophyll *a* are respectively shown in Fig. 7 (middle and right panels) for comparison.

The MERIS monthly mean images (Fig. 7, left panel) show that the maximum chlorophyll *a* concentration in March is found in a coastal region between the Somme and the Scheldt rivers and to the north of the Rhine/Meuse and Thames river mouths. The highest concentrations of the year are seen in April when nearly the entire Southern Bight of the North Sea exhibits high concentration of chlorophyll *a*. From May to July, higher chlorophyll *a* concentrations are restricted to coastal regions with the highest values close to the river mouths. During the summer months, a patch of high chlorophyll *a* concentration with about 50 km diameter is observed in the western Channel at about (49.5°N, 4°W). This has been identified as a bloom of the toxic dinoflagellate *Karenia mikimotoi* (Fernand et al., 2004; Lyons et al., 2004; Vanhoutte-Brunier et al., 2004).

The model results (Fig. 7, middle panel) show a coastal–offshore chlorophyll *a* concentration gradient with higher values near the river mouths and the highest concentrations of the year in April.

The comparison between model results and MERIS data (Fig. 7, right panel) shows a general tendency of the model to underestimate the surface chlorophyll *a* concentration with some exceptions amongst which the more striking are: north of the Scheldt mouth in March, in the Bay of Seine in March and April, in the Thames mouth in May and June, close to the western boundary in March, April and May and in a small area South of UK in March, April and June. The overestimation of the chlorophyll *a* computed by the model seems restricted to areas close to the river mouths and the western boundary. In the French coastal zone, between the Somme estuary and the Belgian waters, there is a significant underestimation in June.

The March–April (resp. June–July) overestimation (resp. underestimation) of the simulated chlorophyll *a* concentration close to the western boundary could be explained by the use of a monthly climatological forcing for the boundary nutrients. The nutrient concentrations (DIN and $PO_4$) imposed at the boundary are on average higher (resp. lower) than *in situ* measurements[1] at the Roscoff ASTAN station (3°56′15″W, 48°46′40″N) in winter and spring (resp. summer). In winter and spring 2003, the mean DIN and $PO_4$ concentrations measured at Roscoff ASTAN were respectively equal to 8.09 mmolN/$m^3$ and 0.32 mmolP/$m^3$. On average, for the same period, the values imposed at the boundary were respectively equal to 9.67 mmolN/$m^3$ and 0.50 mmolP/$m^3$. In summer 2003, the mean DIN and $PO_4$ concentrations measured at Roscoff ASTAN were respectively equal to 2.65 mmolN/$m^3$ and 0.16 mmolP/$m^3$ compared to an average value imposed at the model boundary of 1.71 mmolN/$m^3$ and 0.12 mmolP/$m^3$. A winter–spring (resp. summer) model overestimation (resp. underestimation) of the incoming nutrients could be at the origin of an overestimation (resp. underestimation) of the chlorophyll *a* concentration.

The western Channel summer bloom of *K. mikimotoi*, which is linked to the stratification of surface waters at this time and observed in MERIS images, is not represented by the model. Lack of explicit description of *Karenia* in our model prevents the simulation of their bloom with MIRO. However *Karenia* is a non-siliceous

[1] SOMLIT data provided by the "Service d'Observation en Milieu Littoral", INSU-CNRS, ROSCOFF.

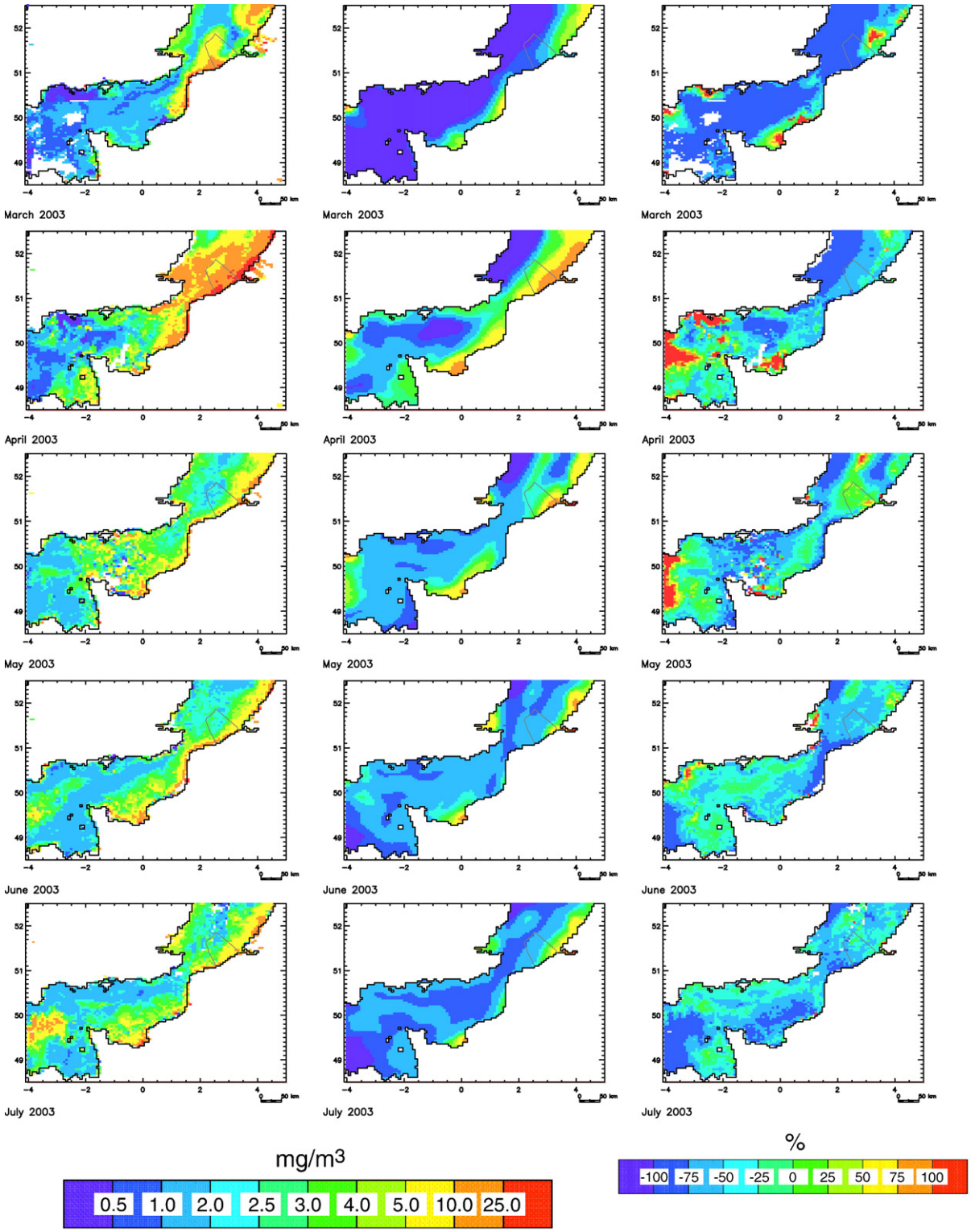


Fig. 7. Left panel: monthly mean chlorophyll *a* derived from MERIS satellite images adapted to the MIRO&CO-3D grid. 69 MERIS images were used for the period of March 2003–July 2003. In average, 2.9 images were valid for a grid cell in these monthly images. Middle panel: monthly mean surface chlorophyll *a* from MIRO&CO-3D. Right panel: monthly mean relative difference ((Model − MERIS) / MERIS * 100) between model and MERIS surface chlorophyll *a*. Positive (resp. negative) values indicate a model overestimation (resp. underestimation). From top to bottom: March 2003–July 2003.

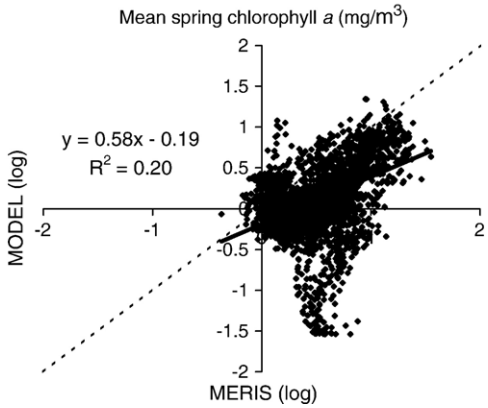


Fig. 8. Scatter plot (log–log) of simulated (*y*-axis) versus MERIS (*x*-axis) chlorophyll *a* concentration (spring 2003) over the whole domain. The solid line corresponds to the regression in the log–log space. The dashed line shows a simulated vs. MERIS chlorophyll *a* concentration ratio of 1.

nanoflagellate which is considered in MIRO. The non-occurrence of a bloom at the time of *Karenia* development means that growth conditions are not fulfilled. Possible reasons are the low vertical resolution of the model (5 levels equally-distant) which prevents a good description of the light field and an accurate representation of the stratification in this area and the proximity of the feature to the model boundary.

The high chlorophyll *a* concentration in the Western part of the Southern Bight of the North Sea in April is not well reproduced by the model, suggesting possibly inadequate boundary conditions for the inflow at the Northwest boundary or the Thames river or overestimation of light limitation. Indeed, significant underestimation of the chlorophyll *a* concentration ($< -75\%$) is generally found in areas where mean model PAR attenuation is very high ($>1\ m^{-1}$). The decrease (from March to July) of the size of the region where the chlorophyll *a* concentration is underestimated by the model could be explained by a delay of the bloom.

A scatter plot with the spring average simulated chlorophyll *a* concentration versus the MERIS chlorophyll *a* is presented in Fig. 8. The analysis of this scatter plot confirms the general tendency of the model to underestimate the surface chlorophyll *a* concentration compared to the MERIS data during the spring bloom. In mean over the spring period (March–April–May), only 9.8% of the simulated chlorophyll *a* is higher than the MERIS one. For respectively 3.6%, 2.3%, 1.3% and 2.6% of the domain, the relative difference between the chlorophyll *a* computed by the model and the MERIS chlorophyll *a* is lower than 25%, between 25% and

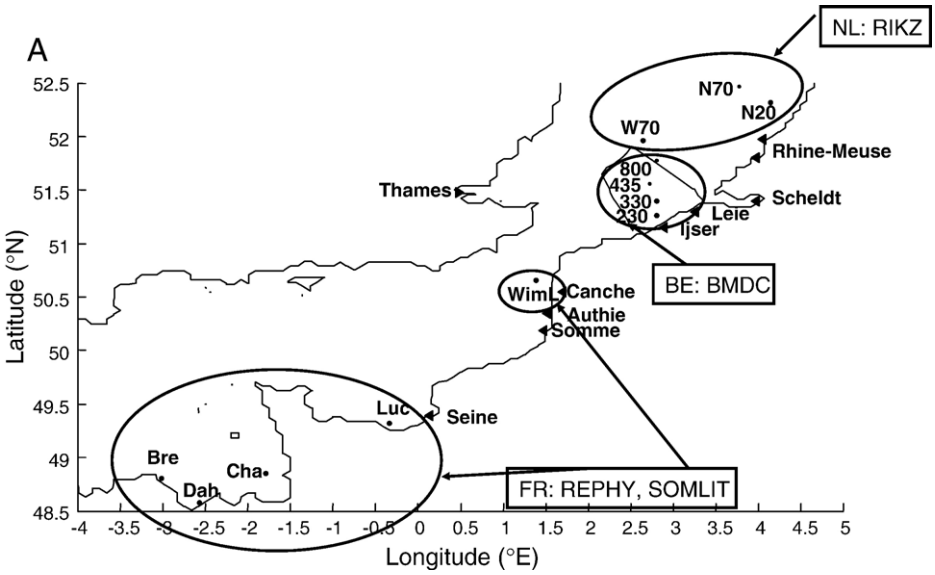


Fig. 9. A. Position of the stations used for comparison between *in situ* modelled and MERIS chlorophyll *a* concentration. RIKZ stations: Noordwijk 20 km (N20), Noordwijk 70 km (N70), Walcheren 70 km (W70). BMDC stations: 230, 330, 435 and 800. REPHY stations: Bouée du Luc 2 milles (Luc), Chausey (Cha), Dahouët (Dah), Bréhat (Bre). SOMLIT station: Wimereux offshore (WimL). Information about the data sources can be found in Table 7. B. Time series of surface chlorophyll *a* for 2003 at some selected stations (see Table 7 and Section 4.4 for choice and data sources and Fig. 9A for position). *In situ* data (black triangles), model results (solid line), MERIS-derived chlorophyll *a* (circles) with minimum and maximum bars corresponding to the different values per grid cell (several MERIS pixels) and per week.

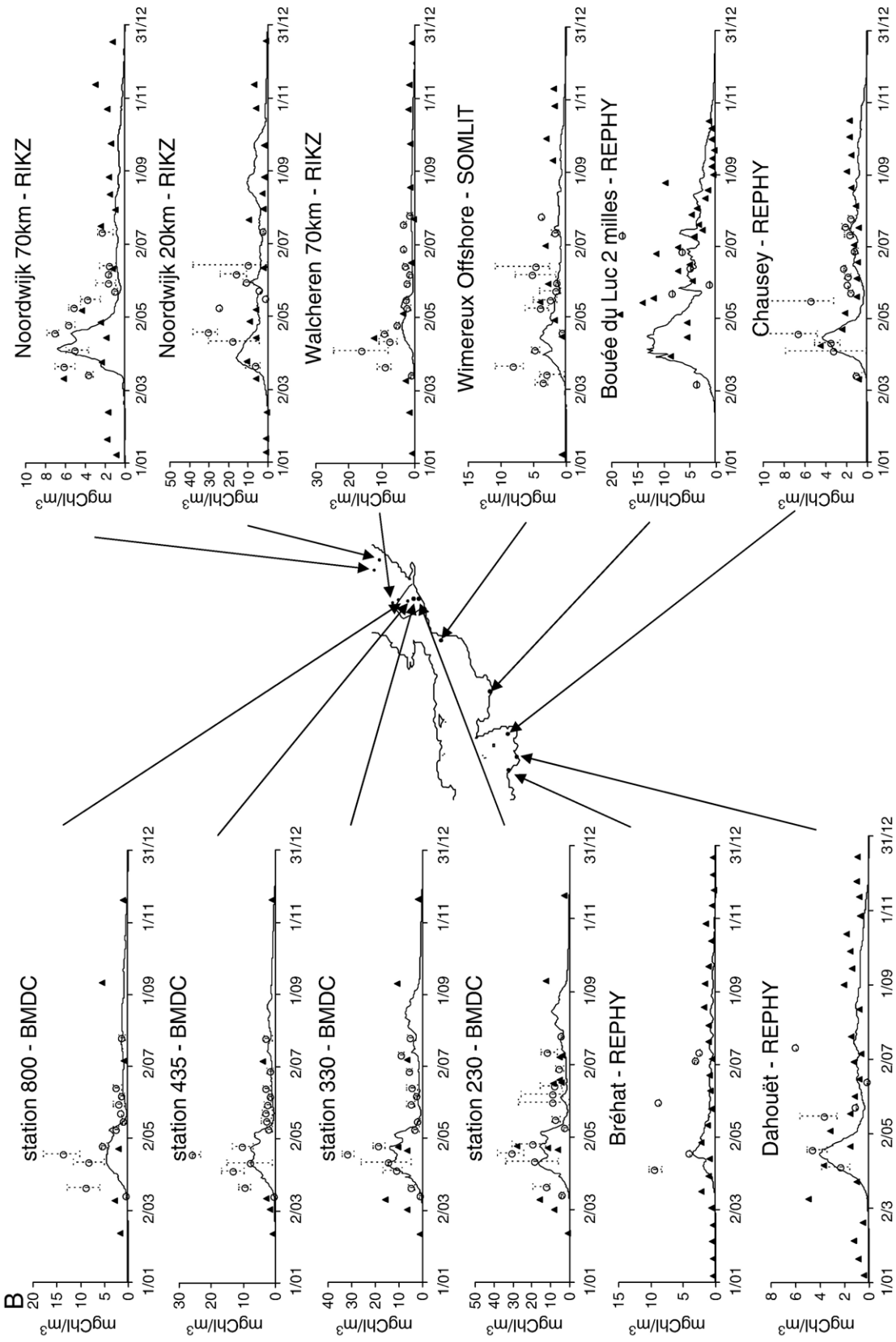


Fig. 9 (*continued*).

Table 7
*In situ* data sets used for surface chlorophyll *a* comparison (2003)

| Data set name | Stations | Source |
|---|---|---|
| BMDC | 230, 330, 435, 800 | Belgian Marine Data Centre. Public data downloaded from the BMDC database http://www.mumm.ac.be/datacentre/ |
| RIKZ | Noordwijk 20 km, Noordwijk 70 km, Walcheren 70 km | Ministry of Transport Public Works and Water Management, National Institute for Coastal and Marine Management / RIKZ, Department of Monitoring and Assessment. Data downloaded from the DONAR database http://www.waterbase.nl. |
| SOMLIT | Wimereux offshore | Data provided by "Service d'Observation en Milieu Littoral (SOMLIT), INSU-CNRS, WIMEREUX" |
| REPHY | Bouée du Luc 2 milles, Chausey, Bréhat, Dahouët | Réseau de Surveillance du Phytoplancton et des Phycotoxines (REPHY), IFREMER. Data downloaded from IFREMER web site http://www.ifremer.fr/envlit/ |

50%, between 50% and 75% and higher than 75%. For 90.2% of the domain the simulated chlorophyll *a* is underestimated. For respectively 8.1%, 22.5%, 39.1% and 20.4% of the domain, the relative difference between the chlorophyll *a* computed by the model and the MERIS chlorophyll *a* is between −25% and 0%, between −50% and −25%, between −75% and −50% and lower than −75%. The lower group of severely underestimated points on this scatter plot are located in the region North and East of the Thames estuary discussed earlier.

Finally a cross comparison between *in situ*, simulated and MERIS-derived surface chlorophyll *a* has been carried out (Fig. 9B) for grid points corresponding to stations sampled by different institutions (Fig. 9A, Table 7). Amongst stations for which *in situ* chlorophyll *a* data were available for the year 2003, a selection has been made in order to cover most of the study region. Stations situated at the limit of the model grid or very close to the border of a grid cell have been eliminated to avoid uncertainties related to strong gradients (especially in coastal region).

The MERIS-derived surface chlorophyll *a* has been averaged horizontally over a grid identical to the model grid and on a weekly basis. The minimum and maximum superimposed bars correspond to the different values per grid cell (several pixels) and per week. Examination of Fig. 9B suggests that the order of magnitude of MERIS-derived chlorophyll *a* is similar to the *in situ* data with nevertheless a tendency to overestimate for some stations (e.g. Bréhat, Chausey, Noordwijk 20 km). For some

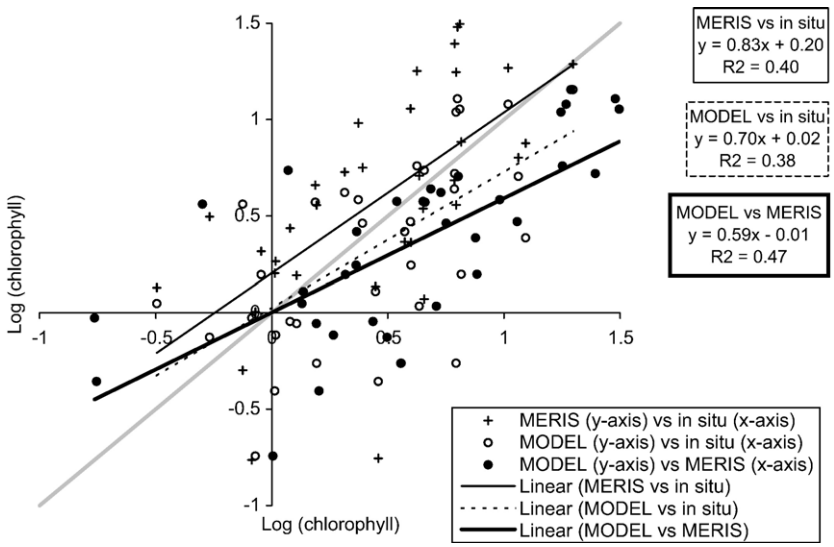


Fig. 10. Scatter plot (log–log) with a two by two comparison of weekly mean simulated chlorophyll *a* weekly mean MERIS chlorophyll *a* and *in situ* chlorophyll *a* concentration (March–July 2003) in mg/m$^3$ for the stations shown in Fig. 9a. The regressions are in the log–log space. The grey line shows a ratio of 1.

stations (e.g. station 230, Noordwijk 20 km, Wimereux offshore, Chausey) the variability (minimum and maximum bars) of MERIS-derived chlorophyll *a* seems very high. The modelled chlorophyll *a* maximum is generally lower than the MERIS-derived chlorophyll *a* except for some stations (e.g. Dahouët, Noordwijk 70 km). Concerning the timing of the bloom the model gives onset in phase with *in situ* and MERIS-derived data for some stations (e.g. Dahouët, Chausey, Noordwijk 20 km) and in phase with only MERIS-derived data for some other stations (e.g. station 330). A delay of the phytoplankton growth as observed in some stations (e.g. station 230) could result from an overestimation of the PAR attenuation that limits light availability. Some simulated chlorophyll *a* peaks have their maxima in phase with data but decrease sooner than in observations (e.g. Dahouët, Noordwijk 70 km) probably as a consequence of nutrient limitation.

To visualize systematic differences between weekly mean MERIS chlorophyll *a* concentration, *in situ* measurements (dates matching within the weeks of MERIS data) and weekly mean simulated chlorophyll *a*, a scatter plot is presented in Fig. 10. This scatter plot allows to compare two by two the MERIS, *in situ* and simulated chlorophyll *a* concentration for the selected stations of Fig. 9. An analysis of this scatter plot shows a general tendency of MERIS to overestimate (resp. underestimate) the surface chlorophyll *a* concentration compared to *in situ* data for concentration lower (resp. higher) than 15 mg/m$^3$. This scatter plot indicates also a general tendency of the model to underestimate (resp. overestimate) the surface chlorophyll *a* concentration compared to *in situ* data for concentration higher (resp. lower) than 1.1 mg/m$^3$ and to underestimate (resp. overestimate) the model chlorophyll *a* concentration compared to MERIS data for concentration higher (resp. lower) than 0.9 mg/m$^3$. Despite these general tendencies there is considerable scatter between the 3 information sources. This can be attributed to both aspects intrinsic to each source and to spatio-temporal sampling difference.

## 5. Discussion–conclusion

The model reproduces well the nitrogen and phosphorus seasonal cycles with nevertheless an underestimation of the DIN decrease due to the low phytoplankton assimilation at the beginning of spring. However, it fails to simulate correctly the dissolved silica cycle, especially during the beginning of spring, due to imperfect representation of the early spring diatom bloom. A sensitivity analysis (not shown) has revealed that the timing of the bloom is extremely sensitive to the available light. Amongst parameters influencing the PAR attenuation coefficient, the non-algae particle concentration is significant. Since that component is estimated from a SeaWiFS TSM seasonal climatology and chlorophyll *a* concentration computed by the model (see Section 2.2), a weakness of the phytoplankton representation and/or the TSM concentration could result in a timing of the bloom discrepancy. TSM concentration is highly variable, especially in the turbid coastal waters of the Belgian and Dutch coasts and in river mouths and the use of a seasonal climatology clearly does not represent tide- and wind-induced high frequency variability. Despite reasonable simulation of nutrients, the chlorophyll *a* maximum is underestimated by the model. One hypothesis for the underestimation of chlorophyll *a* in simulations is a possible overestimation of the loss terms. Mortality (autolysis) and sinking parameters are very difficult to estimate accurately and they are often adjusted in models.

Satellite chlorophyll *a* imagery is shown to be a powerful data source for biogeochemical model validation because of the excellent spatial coverage. However, the removal of unreliable data is important when using satellite chlorophyll *a* data in coastal waters. About 70% of MERIS water pixels were screened using the MERIS product confidence flag in this study. In the context of model validation for regions with varying cloud cover satellite imagery is well adapted for comparison with weekly-averaged or monthly-averaged surface chlorophyll *a* maps. In the present study such an approach showed a good representation by the model of the onshore–offshore chlorophyll *a* gradients associated with riverine nutrient inputs. However, the satellite imagery also reveals new features not picked up by the model such as the bloom of *K. mikimotoi* in the Western Channel (Vanhoutte-Brunier et al., 2004) and the spatial extent of the spring phytoplankton bloom, which covers the entire region from Belgium to South-East England. These differences suggest where further model improvements are necessary. On the other hand the satellite imagery has itself a number of limitations where improvements are also necessary. Comparison with *in situ* measurements suggests a tendency for overestimation of surface chlorophyll *a* by MERIS. Possible causes include imperfect atmospheric correction (Doerffer et al., 2003) or underestimation of the chlorophyll-specific phytoplankton absorption coefficient used to convert (European Space Agency, 2001) from the optical property, absorption, to the geophysical parameter, chlorophyll *a*. Another limitation is the reduced number of images available. This was insufficient here for validation of the model results as regards timing and duration of bloom events and in some cases led to weekly- or monthly-averages being based on only one or two days'

observations. In the long term the frequency of available imagery could be improved by combining data from satellites with different overpass times (provided data quality is acceptable), and by the use of future geostationary satellites and/or tilted sensors which avoid sun glint. For an accurate assessment of the timing and duration of blooms (but not of absolute chlorophyll *a* concentrations) the use of very high frequency measurements from moored fluorimeters (Mills et al., 1994) is recommended.

This validation shows that the MIRO&CO-3D model can reproduce with relatively good accuracy the seasonal dynamics of chlorophyll *a* and nutrients. In a recent review, Radach and Moll (2006) have shown that all North Sea ecosystem models have at least one state variable not realistically simulated (from the point of view of seasonal dynamics) and cannot reproduce with accuracy the spring chlorophyll *a* spatial distribution. From their comparison between simulated and observed annual cycles they also concluded that in general the nutrients phosphate and silicate were simulated best, with less success for nitrogen nutrients. Chlorophyll *a* was simulated to an order of magnitude, sometimes over-, sometimes underestimated. Compared to their analysis, the performances of MIRO&CO-3D seem at least comparable to other models except that it is the simulated silica that appears to be least reliable.

In this paper the "visual based" validation presented has been enhanced by a quantitative/objective validation of the model as suggested by Radach and Moll (2006). The validation exercise presented here is however far from complete and one future step in the validation procedure would be to compare simulated fluxes (e.g. primary production) with data. Available flux data is currently sparse but could be significantly enhanced by development of suitable remotely sensed products.

## Acknowledgement

This work has been carried out in the scope of the AMORE-II project (EV/36/19B) funded by the Belgian Federal Science Policy Office in the framework of the "Scientific Support Plan for a Sustainable Development Policy — Sustainable Management of the North Sea". The CAMME team is acknowledged for computing support. MERIS data used here was supplied by the European Space Agency under Envisat AOID698 and processing was carried out in the scope of the BELCOLOUR project funded by the STEREO programme of the Belgian Federal Science Policy Office. Yvette Spitz is acknowledged for fruitful discussions during the model development phase. Two anonymous referees and A. Ménesguen are acknowledged for their constructive suggestions.

## References

Allen, J.I., Blackford, J., Holt, J., Proctor, R., Ashworth, M., Siddorn, J., 2001. A highly spatially resolved ecosystem model for the North West European Continental Shelf. Sarsia 86, 423–440.

Baretta, J.W., Ebenhoeh, W., Ruardij, P., 1995. The European Regional Seas Ecosystem Model, a complex marine ecosystem model. Netherlands Journal of Sea Research 33 (3–4), 233–246.

Billen, G., Servais, P., 1989. Modélisation des processus de dégradation bactérienne de la matière organique en milieu aquatique. In: Bianchi, M., Marty, D., Bertrand, J.C., Caumette, P., Gauthier, M. (Eds.), Microorganismes dans les écosystèmes océaniques. Masson, Paris, pp. 219–245.

Billen, G., Dessery, S., Lancelot, C., Meybeck, M., 1989. Seasonal and interannual variations of nitrogen diagenesis in the sediments of a recently impounded basin. Biogeochemistry 8, 73–100.

Buiteveld, H., 1995. A model for calculation of diffuse light attenuation (PAR) and Secchi depth. Netherlands Journal of Aquatic Ecology 29 (1), 55–65.

Cugier, P., Billen, G., Guillaud, J.F., Garnier, J., Ménesguen, A., 2005. Modelling of eutrophication of the Seine Bight (France) under historical, present and future riverine nutrient loading. Journal of Hydrology 304, 381–396.

Damm, P., 1989. Klimatologischer Atlas des Salzgehalted, der Temperatur und der Dichte in der Nordsee, 1968–1985. 6-89, Institut für Meereskunde der Universität Hamburg, Hamburg.

Deleersnijder, E., Wolanski, E., Norro, A., 1989. Numerical simulation of the three-dimensional tidal circulation in an island's wake. In: Carlomango, G.M., Brebbia, C.A. (Eds.), Computers and experiments in fluid flow. Springer-Verlag, pp. 355–381.

Delhez, E.J.M., 1998. Macroscale ecohydrodynamic modeling on the northwest European continental shelf. Journal of Marine Systems 16, 171–190.

Doerffer, R., Schiller, H., Krasemann, H., Heymann, K., Cordes, W., Schönfeld, W., Röttgers, R., Behner, I., Kipp, P., 2003. MERIS Case 2 Water Validation Early Results North Sea/Hegoland/German Bight, Envisat Validation workshop, 9–13th December 2002. European Space Agency, Frascati.

European Space Agency, 2001. Reference model for MERIS Level 2 Processing (Chapter 4). issue 4.

Fernand, L., McCloghrie, P., Raine, R., Lyons, S., Chambers, C., Cussack, C., Wooltorton, J., 2004. Circulation of the western English Channel: a combination of factors. Abstract of the Presentation at the "Challenger conference for marine science", Liverpool, 13–17 September 2004. http://www.ifremer.fr/delec/projets/efflores_phyto/phaeocystis/poster_liverpool.pdf.

Gons, H.J., Rijkeboer, M., Ruddick, K.G., 2005. Effect of a waveband shift on chlorophyll retrieval from MERIS imagery of inland and coastal waters. Journal of Plankton Research 27 (1), 125–127.

Lacroix, G., Ruddick, K.G., Ozer, J., Lancelot, C., 2004. Modelling the impact of the Scheldt and Rhine/Meuse plumes on the salinity distribution in Belgian waters (southern North Sea). Journal of Sea Research 52 (3), 149–163.

Lancelot-Van Beveren, C., 1980. A statistical method to estimate the biochemical composition of phytoplankton in the Southern Bight of the North Sea. Estuarine and Coastal Marine Science 10, 467–478.

Lancelot, C., Billen, G., 1985. Carbon–nitrogen relationships in nutrient metabolism of coastal marine ecosystems. Advances in Aquatic Microbiology 3, 263–321.

Lancelot, C., Billen, G., Sournia, A., Weisse, T., Colijn, F., Veldhuis, M.J.W., Davies, A., Wassman, P., 1987. *Phaeocystis* blooms and nutrient

enrichment in the continental coastal zones of the North Sea. Ambio 16 (1), 38–46.

Lancelot, C., Rousseau, V., Becquevort, S., Parent, J.Y., et al., 2004. Study and modelling of eutrophication-related changes in coastal planktonic food-webs: a contribution of the AMORE (Advanced Modeling and Research on Eutrophication) consortium. Final report. Scientific Support Plan for a Sustainable Development Policy–Sustainable Management of the North Sea. Belgian Science Policy, Brussels.

Lancelot, C., Spitz, Y., Gypens, N., Ruddick, K., Becquevort, S., Rousseau, V., Lacroix, G., Billen, G., 2005. Modelling diatom and *Phaeocystis* blooms and nutrient cycles in the Southern Bight of the North Sea: the MIRO model. Marine Ecology Progress Series 289, 63–78.

Lancelot, C., Veth, C., Mathot, S., 1991. Modelling ice edge phytoplankton bloom in the Scotia–Weddell Sea sector of the Southern Ocean during spring 1988. Journal of Marine Systems 2, 333–346.

Loewe, P., 2003. Weekly North Sea SST Analyses since 1968. In: Hydrographie, O.d.a.h.b.B.f.S.u. (Ed.), D-20305 Hamburg, P.O. Box 301220, Germany.

Luyten, P.J., Jones, J.E., Proctor, R., Tabor, A., Tett, P., Wild-Allen, K., 1999. COHERENS Documentation: a Coupled Hydrodynamical-Ecological Model for Regional and Shelf Seas: User Documentation. MUMM, Brussels.

Lyons, S., Chambers, C., Raine, R., Fernand, L., 2004. *Karenia mikimotoi* populations in the western English Channel. Abstract of the Presentation at the "Challenger Conference for Marine Science", Liverpool, 13–17 September 2004. http://www.ifremer.fr/delec/projets/efflores_phyto/phaeocystis/poster_liverpool.pdf.

Ménesguen, A., Hoch, T., 1997. Modelling the biogeochemical cycles of elements limiting primary production in the English Channel. 1. Role of thermohaline stratification. Marine Ecology Progress Series 146 (1–3), 173–188.

Mills, D.K., Tett, P.B., Novarino, G., 1994. The spring bloom in the South Western North Sea in 1989. Netherlands Journal of Sea Research 33 (1), 65–80.

Moll, A., 1997. Modelling primary production in the North Sea. Oceanography 10 (1), 24–26.

Moll, A., 1998. Regional distribution of primary production in the North Sea simulated by a three-dimensional model. Journal of Marine Systems 16, 151–170.

Moll, A., Radach, G., 2003. Review of three-dimensional ecological modelling related to the North Sea shelf system. Part 1: models and their results. Progress in Oceanography 57, 175–217.

Moore, G.F., Aiken, J., Lavender, S.J., 1999. The atmospheric correction of water colour and the quantitative retrieval of suspended particulate matter in Case II waters: application to MERIS. International Journal of Remote Sensing 20 (9), 1713–1734.

Morel, A., 1988. Optical modelling of the upper ocean in relation to its biogenous matter content (Case I waters). Journal of Geophysical Research 93, 10749–10768.

Nechad, B., De Cauwer, V., Park, Y., Ruddick, K., 2003. Suspended Particulate Matter (SPM) mapping from MERIS imagery. Calibration of a Regional Algorithm for the Belgian Coastal Waters, MERIS User Workshop, 10–13th November 2003. European Space Agency, Frascati.

OSPAR, Villars, M., Vries, I.d., Bokhorst, M., Ferreira, J., Gellers-Barkman, S., Kelly-Gerreyn, B., Lancelot, C., Ménesguen, A., Moll, A., Pätsch, J., Radach, G., Skogen, M., Soiland, H., Svendsen, E. and Vested, H.J., 1998. Report of the ASMO modelling workshop on eutrophication Issues, 5–8 November 1996. The Hague, The Netherlands. OSPAR Commission Report, RIKZ, The Hague: 102.

Park, Y., De Cauwer, V., Nechad, B., Ruddick, K., 2003. Validation of MERIS water products for Belgian coastal waters: 2002–2003. MERIS and AATSR Calibration and Geophysical Validation workshop, 20–24th October 2003. European Space Agency, Frascati.

Pätsch, J., Radach, G., 1997. Long-term simulation of the eutrophication of the North Sea: temporal development of nutrients, chlorophyll and primary production in comparison to observations. Journal of Sea Research 38 (3–4), 275–310.

Radach, G., Lenhart, H.J., 1995. Nutrient dynamics in the North Sea: fluxes and budgets in the water column derived from ERSEM. Netherlands Journal of Sea Research 33 (3–4), 301–335.

Radach, G., Moll, A., 2006. Review of three-dimensional ecological modelling related to the North Sea shelf system—Part 2: model validation and data needs. Oceanography and Marine Biology; An Annual Review 44, 1–60.

Riegman, R., Noordeloos, A.A.M., Cadée, G.C., 1992. *Phaeocystis* blooms and eutrophication of the continental coast zones of the North Sea. Marine Biology 112, 479–484.

Rijkswaterstaat, T.W.D., 1992. Guidance document for the NSTF modelling workshop 6–8th May, 1992, Hague.

Rousseau, V., 2000. Dynamics of *Phaeocystis* and diatom blooms in the eutrophicated coastal waters of the Southern Bight of the North Sea. PhD Thesis Thesis, Université Libre de Bruxelles.

Rousseau, V., Breton, E., De Wachter, B., Beji, A., Deconinck, M., Huijgh, J., Bolsens, T., Leroy, D., Lancelot, C., 2002a. IZEUT: identification of Belgian maritime zones affected by eutrophication. Implementation of the OSPAR Comman Procedure to combat eutrophication. Final report.

Rousseau, V., Leynaert, A., Daoud, N., Lancelot, C., 2002b. Diatom succession, silicification and silicic acid availability in Belgian coastal waters (southern North Sea). Marine Ecology Progress Series 236, 61–73.

Ruddick, K.G., 1995. Modelling of coastal processes influenced by the freshwater discharge of the Rhine. PhD Thesis, Université de Liège, 247 pp.

Ruddick, K.G., Ovidio, F., Vasilkov, A., Lancelot, C., Rousseau, V., Rijkeboer, M., 1999. Optical remote sensing in support of eutrophication monitoring in Belgian waters. In: Nieuwenhuis, G.J.A., Vaughan, R.A., Molenaar, M. (Eds.), 18th EARSEL Symposium on Operational Remote Sensing for Sustainable Development. A.A. Balkema, Rotterdam, Enschede, pp. 445–452.

Schiller, H., Doerffer, R., 1999. Neural network for emulation of an inverse model operational derivation of Case II water properties from MERIS data. International Journal of Remote Sensing 20 (9), 1735–1746.

Skogen, M., Moll, A., 2005. Importance of ocean circulation in ecological modelling: an example from the North Sea. Journal of Marine Systems 57 (3–4), 289–300.

Skogen, M.D., Aure, J., Danielssen, D., Svendsen, E., 1998. Natural fertilisation of the marine environment-modelling of the Gomma Flood 1995. Sarsia 83, 361–372.

Skogen, M.D., Soiland, H., 1998. A User's Guide to NORWECOM v2, the Norwegian Ecological Model System. Institute of Marine Research, Bergen.

Skogen, M.D., Svendsen, E., Berntsen, J., Aksnes, D., Ulvestad, K.B., 1995. Modelling the primary production in the North Sea using a coupled 3-dimensional physical chemical biological ocean model. Estuarine, Coastal and Shelf Science 41, 545–565.

Vanhoutte-Brunier, A., Lyons, S., Fernand, L., Cugier, P., Dumas, F., Menesguen, A., Gohin, F., 2004. Modelling harmful algal events in the western English Channel applied to the *Karenia mikimotoi* bloom that occurred in summer 2003. Abstract of the Presentation at the "Challenger Conference for Marine Science", Liverpool,

13–17 September 2004. http://www.ifremer.fr/delec/projets/efflores_phyto/phaeocystis/poster_liverpool.pdf.

Veldhuis, M.J.W., Colijn, F., Venekamp, L.A.H., 1986. The spring bloom of *Phaeocystis pouchetti* (Haptophycea) in Dutch coastal waters. Netherlands Journal of Sea Research 20, 37–48.

Vichi, M., Baretta, J.W., Baretta-Bekker, J.G., Ebenhöh, W., Kohlmeier, C., Ruardij, P., Pinardi, N., Zavatarelli, M., 2004. European Regional Seas Ecosystem Model III. Review of the biogeochemical equations. Documentation Release Version: 3.4-Alpha $Id:ERSEM_III_report.lyx,v 1.6 2004/07/28 10:44:29 mav Exp. $. 88 pp.